HHS Public Access
Author manuscript
Circ Res. Author manuscript; available in PMC 2016 May 25.

Published in final edited form as:
Circ Res. 2010 June 25; 106(12): 1893–1903. doi:10.1161/CIRCRESAHA.110.220855.

Intramyocardial VEGF-B_{167} Gene Delivery Delays the Progression Towards Congestive Failure in Dogs With Pacing-Induced Dilated Cardiomyopathy

Martino Pepe[*], **Mohammed Mamdani**[*], **Lorena Zentilin**[*], **Anna Csiszar**, **Khaled Qanud**, **Serena Zacchigna**, **Zoltan Ungvari**, **Uday Puligadda**, **Silvia Moimas**, **Xiaobin Xu**, **John G. Edwards**, **Thomas H. Hintze**, **Mauro Giacca**, and **Fabio A. Recchia**
Department of Physiology (M.P., M.M., K.Q., X.X., J.G.E., T.H.H., F.A.R.), New York Medical College, Valhalla, NY; International Centre for Genetic Engineering and Biotechnology (L.Z., S.Z., U.P., S.M., M.G.), Trieste, Italy; Reynolds Oklahoma Center on Aging (A.C., Z.U.), Department of Geriatric Medicine, University of Oklahoma Health Science Center, Oklahoma City; and Sector of Medicine (F.A.R.), Scuola Superiore Sant'Anna, Pisa, Italy

Abstract

Rationale—Vascular endothelial growth factor (VEGF)-B selectively binds VEGF receptor (VEGFR)-1, a receptor that does not mediate angiogenesis, and is emerging as a major cytoprotective factor.

Objective—To test the hypothesis that VEGF-B exerts non–angiogenesis-related cardioprotective effects in nonischemic dilated cardiomyopathy.

Methods and Results—AAV-9–carried VEGF-B_{167} cDNA (10^{12} genome copies) was injected into the myocardium of chronically instrumented dogs developing tachypacing-induced dilated cardiomyopathy. After 4 weeks of pacing, green fluorescent protein–transduced dogs (AAV-control, n=8) were in overt congestive heart failure, whereas the VEGF-B–transduced (AAV-VEGF-B, n=8) were still in a well-compensated state, with physiological arterial P_{O_2}. Left ventricular (LV) end-diastolic pressure in AAV-VEGF-B and AAV-control was, respectively, 15.0±1.5 versus 26.7±1.8 mm Hg and LV regional fractional shortening was 9.4±1.6% versus 3.0±0.6% (all $P<0.05$). VEGF-B prevented LV wall thinning but did not induce cardiac hypertrophy and did not affect the density of α-smooth muscle actin–positive microvessels, whereas it normalized TUNEL-positive cardiomyocytes and caspase-9 and -3 activation. Consistently, activated Akt, a major negative regulator of apoptosis, was superphysiological in AAV-VEGF-B, whereas the proapoptotic intracellular mediators glycogen synthase kinase (GSK)-3β and FoxO3a (Akt targets) were activated in AAV-control, but not in AAV-VEGF-B. Cardiac VEGFR-1 expression was reduced 4-fold in all paced dogs, suggesting that exogenous VEGF-B_{167} exerted a compensatory receptor stimulation. The cytoprotective effects of VEGF-

Correspondence to: Fabio A. Recchia, MD, PhD, Department of Physiology, New York Medical College, Valhalla, NY 10595. ; Email: fabio_recchia@nymc.edu
[*]These authors contributed equally to this work.

Disclosures
None.

B$_{167}$ were further elucidated in cultured rat neonatal cardiomyocytes exposed to 10^{-8} mol/L angiotensin II: VEGF-B$_{167}$ prevented oxidative stress, loss of mitochondrial membrane potential, and, consequently, apoptosis.

Conclusions—We determined a novel, angiogenesis-unrelated cardioprotective effect of VEGF-B$_{167}$ in nonischemic dilated cardiomyopathy, which limits apoptotic cell loss and delays the progression toward failure.

Keywords

heart failure; vascular endothelial growth factors; gene therapy

---

Vascular endothelial growth factor (VEGF)-B, 1 of the 5 members of the VEGF family,[1] is relatively understudied compared to VEGF-A, yet is emerging as a major cytoprotective factor.[2,3] Expressed in tissues with elevated metabolism, including myocardium,[4] the VEGF-B gene encodes for 2 isoforms, VEGF-B$_{167}$ and VEGF-B$_{186}$, which selectively bind the receptors VEGFR-1 and neuropilin-1.[4,5] Based on data from knockout and transgenic animals, this growth factor is minimally angiogenic and its absence is compatible with birth and growth, although it seems important for physiological cardiac development.[6–8] Li et al have recently elucidated mechanisms responsible for VEGF-B–induced cytoprotection: VEGF-B$_{167}$, via VEGFR-1, down-regulates genes of the apoptosis/cell death-related pathways, in vitro, and can rescue neurons from apoptosis in mouse models of retinal and brain damage.[2] The same authors found that, under pathological conditions, VEGF-B$_{167}$, albeit unable to induce blood vessel growth, is critically required for the survival of newly formed vascular cells.[3] We have later shown that VEGF-B$_{167}$ gene transfer in infarcted rat hearts attenuates remodeling and preserves viable cardiac tissue and contractility in the absence of significant induction of angiogenesis. [9] This is suggestive of an angiogenesis-unrelated, direct prosurvival effect of VEGF-B$_{167}$ on cardiomyocytes; however, no studies, to date, have tested a similar protective role in cardiac diseases, such as dilated cardiomyopathy, not associated with major vasculopathic/ischemic events. Although it is not the principal cause of heart failure, dilated cardiomyopathy is particularly malignant, accounting for the majority of cardiac transplants in the US,[10] and its underlying etiology remains in most cases undetermined. By definition, dilated cardiomyopathy is not caused by large necrotic tissue loss consequent to coronary artery disease; hence, it would not benefit from neoangiogenesis, whereas it is characterized by modest and widespread myocardial fibrosis and increased apoptosis.[11,12] Interestingly, a clinical study found that in dilated, but not in ischemic cardiomyopathy, a higher rate of apoptosis was associated with a more rapidly deteriorating clinical course.[13] Moreover, experimental studies have shown that a few hundred apoptotic cells per million are sufficient to cause dilated cardiomyopathy, which can be prevented by halting the mechanisms of cell death.[14,15] It is also noteworthy that cardiac VEGRF-1 expression is downregulated in patients with dilated, but not ischemic cardiomyopathy.[16] Based on these observations, we tested the hypothesis that VEGF-B$_{167}$ overexpression can attenuate the structural and functional derangement of cardiac muscle in dilated cardiomyopathy. Our study was conducted in canine pacing-induced heart failure, which remains to date one of the best available preclinical models of human dilated cardiomyopathy. The prevalence of apoptosis in dog hearts subjected to sustained tachypacing is similar to that found in patients,[17] and the time course of failure is very predictable; therefore, this model is well-suited to test potential cytoprotective and protrophic effects of VEGF-B_{167} delivery. To obtain sustained expression over time, VEGF-B_{167} gene transfer was performed by using recombinant adeno-associated virus of serotype 9 (AAV9), a vector with marked cardiotropism.[18] Mechanisms of cell protection were further tested in cultured cardiomyocytes.

Methods

An expanded Methods section is available in the Online Data Supplement at http://circres.ahajournals.org.

Surgical Instrumentation and AAV Delivery

Twenty-two adult, male, mongrel dogs (25 to 27 kg) were chronically instrumented as previously described.[19,20] In addition, 2 pairs of piezoelectric crystals were implanted in the midmyocardium of the left ventricular (LV) free wall, orthogonal to the ventricular long axis, 10 to 15 mm apart, to assess regional circumferential shortening. During surgery and following a random order, in 14 dogs the heart was transduced with VEGF-B_{167} and in 8 dogs with the green fluorescent protein (GFP) transgene by 10 intramyocardial injections of 0.1 mL of AAV9 vectors (0.5×10^{11} genome copies per injection) into the LV free wall, according to a predefined map (Online Figure I). Some of the points of injection were previously tagged with epicardial thick silk stitches to allow postmortem identification of the spots. One injection was performed in between each of the 2 pairs of piezoelectric crystals.

Experimental Protocol

Ten to 12 days after surgery and AAV delivery, baseline hemodynamics, regional shortening, echocardiographic measurements were taken and paired arterial and coronary sinus blood samples collected in conscious, nonsedated animals, trained to lie down quietly and unrestrained on the laboratory table. Data were taken at spontaneous heart rate and after 10 minutes pacing at 210 bpm. Absolute myocardial flow was measured by injecting stable isotope-labeled microspheres, both at spontaneous heart rate and during pacing.[21] After these baseline measurements, 8 of the 14 VEGF-B_{167}–transduced (AAV-VEGF-B group) and the 8 GFP-transduced dogs (AAV-control group) were subjected to chronic LV pacing at 210 bpm for 3 weeks; then the rate was increases to 240 bpm for an additional week. The same measurements performed at baseline (0 weeks pacing) were repeated at 3 and 4 weeks of pacing, except for the microsphere injection and paired arterial and coronary sinus blood sampling, which were repeated only at 4 weeks when the protocol was completed. Based on our previous studies in dogs undergoing this pacing protocol, at 3 weeks dogs are still in compensated failure,[19,20] whereas at 4 weeks they reach end-stage heart failure, characterized by a LV end-diastolic pressure of ≥25 mm Hg, drop in arterial P_{O_2}, and dyspnea. The remaining 6 VEGF-B_{167}-transduced dogs were monitored for 4 weeks but not paced and used to assess potential functional and morphological changes attributable to long-term VEGF-B_{167} overexpression in a normal heart (AAV-VEGF-B nonpaced group).

At the completion of the protocol, the dogs were euthanized with an overdose of sodium pentobarbital, the heart was weighed, and transmural LV tissue samples were harvested from the AAV-injected spots, ie, the anterolateral LV free wall, and from the remote LV region, ie, the posterolateral LV free wall, close to the left posterior descending coronary artery. They were immediately stored in liquid nitrogen or phosphate 10% formalin and coded for blinded molecular and histological analysis, or exsiccated for later counting of the microspheres. Only for comparisons of macroscopic (cardiac weight) and histological cardiac changes, we used data and tissue samples obtained from a further group of 5 healthy dogs that, after full recovery from chronic instrumentation, were euthanized because of major failures of the implanted probes. This group is indicated as “normal.”

Surgical instrumentation and protocol were approved by the Institutional Animal Care and Use Committee of the New York Medical College and conform to the guiding principles for the care and use of laboratory animals published by the National Institutes of Health.

Hemodynamics, LV Regional Shortening, Echocardiographic Recordings and MVO_2

See the Online Data Supplement.

Production, Purification, and Characterization of Recombinant AAV Vectors

Mouse VEGF-B_{167} cDNA was incorporated into recombinant AAV-9 prepared by the AAV Vector Unit at ICGEB Trieste (http://www.icgeb.org/avu-core-facility.html), by a cross-packaging approach whereby the AAV type 2 vector genome was packaged into AAV capsid serotype 9. Methods for production and purification were previously described.[22] AAV titers were in the range of 1×10^{12} genome copies per milliliter.

Histology and Immunofluorescence

To determine alterations in microvascular density, endothelial cells were detected using FITC-conjugated *Lycopersicum esculentum* lectin and vascular smooth muscle cells using a Cy3-conjugated anti α-SMA mouse monoclonal antibody. The microvessel number was normalized by the number of cardiac fibers. Apoptotic cells were visualized by TUNEL and cardiomyocyte cross-sectional area was measured.[9,22]

Isoprostane and Caspase-9 Activity in LV Tissue

Because the production of reactive oxygen species is increased in the failing heart,[23,24] we measured 8-isoprostane content, an index of oxidative stress, and the activity of caspase-9, which increases in response to oxidative mitochondrial damage, thus triggering the apoptotic cascade. In LV tissue homogenates, 8-isoprostane was measured by the EIA kit (Cayman Chemicals) and caspase-9 activity in LV homogenates was measured with a colorimetric activity assay kit.

PCR, ELISA, and Western Blotting

Total LV DNA was extracted to detect AAV genomic DNA and RNA was purified to quantify murine VEGF-B_{167} (AAV-carried transgene) and dog VEGF-B_{167}, VEGF-A_{165}, VEGFR-1, VEGFR-2 and Neuropilin-1 transcripts. Dog serum samples from arterial and coronary sinus blood were analyzed by ELISA for the presence of mouse VEGF-B_{167}

secreted in the circulation from the transduced heart tissue. Western blot was used to quantify the activated/cleaved caspase-3, which is the final common effector of the apoptotic pathway, and to determine the activation state of Akt, a major antiapoptotic kinase,[25] and of 2 of its targets critically involved in the positive regulation of apoptosis, namely GSK-3β and FoxO3a, which are inactivated by phosphorylation in the cytosol and in the nucleus, respectively.[26–28]

Cultured Cardiac Myocytes

Potential mechanisms of cytoprotection mediated by VEGF-B_{167} were studied in neonatal rat cardiomyocytes. There are many causes of cell damage occurring in the failing heart, still partially unknown, therefore we focused on a major one, namely the upregulated angiotensin II (Ang II),[29] one of the main activators of oxidative stress.[30] Cardiomyocytes were cultured and pretreated with murine VEGF-B_{167} protein (100 ng/mL, for 24 hour) or vehicle. Then the culture medium was added with Ang II (10^{-8} mol/L, for 24 hour). After the treatment period the percent of TUNEL-positive cells, a marker of apoptosis, and caspase-3 and -9 activities were assessed in cell homogenates.

To elucidate downstream effects of Ang II, we tested Ang II–induced mitochondrial $O_2^{\cdot-}$ production and consequent damage.[31] Neonatal rat cardiomyocytes were exposed to Ang II with and without VEGF-B_{167} as described above. We then assessed Ang II–induced mitochondrial $O_2^{\cdot-}$ production and total cell peroxide production. Changes in mitochondrial membrane potential were measured as they are a known downstream effect of Ang II–induced oxidative stress. We have used these methods previously.[32]

Statistical Analysis

Data are presented as means±SEM. Statistical analysis was performed by using commercially available software. Changes at different time points in the same group and differences among groups or in vitro data sets were compared by one- and two-way ANOVA followed by Tukey post hoc test. For all of the statistical analyses, significance was accepted at $P<0.05$.

Results

Hemodynamics

The hemodynamic changes found in AAV-control were very consistent with the typical evolution of this model of failure, as previously described by us.[18,19] LV end-diastolic pressure (Figure 1) reached values ≥25 mm Hg after 4 weeks of pacing, indicating a condition of end-stage, congestive heart failure. However, VEGF-B_{167} delivery markedly attenuated this increase, and, at 4 weeks, LV end-diastolic pressure was still comparable to values found at 3 weeks in AAV-control. Consistent with the development of congestive heart failure, in AAV-control arterial P_{O_2} decreased from 90.0±2.9 mm Hg at baseline (P=NS versus the AAV-VEGF-B group) to 67.0±4.8 mm Hg after 4 weeks of pacing ($P<0.05$ versus baseline), whereas the better preserved diastolic function in the AAV-VEGF-B group was reflected by an arterial P_{O_2} of 83.4±5.2 mm Hg at 4 weeks (P=NS versus baseline).

Figure 1 shows other major hemodynamic changes. Compared to AAV-control, VEGF-B gene delivery limited the fall in LV systolic pressure, dP/dt_{max} and mean arterial pressure during the pacing protocol. On the other hand, there were no significant hemodynamic changes from baseline during the 4-week follow up in the AAV-VEGF-B nonpaced group (data not shown).

Global and Regional Cardiac Function

Global cardiac function was evaluated by echocardiography (Figure 2). Ejection fraction decreased significantly in both groups, although it was better preserved in AAV-VEGF-B. LV end-diastolic diameter increased significantly only in AAV-control; however, the same trend was also present in AAV-VEGF-B, and therefore there was no significant difference between the 2 groups. LV end-systolic diameter increased significantly in both groups. Two parameters that did not change significantly in AAV-VEGF-B during the pacing protocol were the end-diastolic thickness and systolic thickening of the LV free wall. As expected, there were significant LV wall thinning and diminished systolic thickening in AAV-control. Thickening is an index of regional contractile performance that we measured along the selected plane of echo scanning. To further explore regional changes in contractile performance of the transduced LV areas, we measured circumferential systolic shortening with piezoelectric crystals (Figure 3), which, consistent with the echo data, decreased significantly in AAV-control, but was markedly preserved in AAV-VEGF-B. The integral of the LV pressure-segmental length loop provides a surrogate of regional stroke work, that, expressed as a percentage of the baseline (0 weeks), fell significantly by approximately 89% in AAV-control, but only by 58% in AAV-VEGF-B, after 4 weeks of pacing. Figure 3B shows 2 examples of changes in the pressure-length loops in the 2 groups, with the remarkable preservation of regional function in AAV-VEGF-B. Please note that the different baseline loops in the 2 groups were attributable to the unavoidable variability, from dog to dog, of the distance between crystals placed during surgery, and for that reason regional work in Figure 3A is expressed as percentage of baseline. On the other hand, there were no significant changes from baseline, in wall thickness and global and regional function, during the 4-week follow up in the AAV-VEGF-B nonpaced group (data not shown).

Coronary Flow and MVO_2

The beneficial effects of AAV-VEGF-B delivery could be possibly attributable to myocardial neoangiogenesis and therefore enhanced blood perfusion and oxygen consumption. We therefore measured coronary blood flow in the circumflex coronary artery, which is responsible for the perfusion of a large portion of the LV free wall, including the transduced areas. Moreover, we measured absolute myocardial perfusion in samples selectively taken from the AAV-injected spots. As shown in the Table, no significant differences were found between the 2 groups, both at spontaneous heart rate and during acute pacing stress, at baseline and after 4 weeks of pacing. MVO_2 displayed a trend toward increased baseline values in AAV-VEGF-B compared to AAV-control; however, these differences between the 2 groups were not statistical significant, not even during acute pacing stress.

Structural Changes at Macroscopic and Microscopic Level

The heart weight to body weight ratio was 10.07±0.29 g/kg in AAV-VEGF-B, 9.07±0.36 g/kg in AAV-control, 9.04±0.17 g/kg in nonpaced AAV-VEGF-B and 9.21±0.22 g/kg in normal (*P*=NS for all comparisons). Histology revealed an approximately 15% reduction in capillary density in AAV-control compared to normal, which was prevented in AAV-VEGF-B (Figure 4A and 4B). On the other hand, the density of microvessels with α-smooth muscle actin positive wall was not significantly different among groups (Figure 4A and 4C). Cardiomyocytes cross-sectional area was significantly increased in both paced and nonpaced AAV-VEGF-B compared to normal (Figure 4D and 4E), a local effect limited to the site of injection that was evidently insufficient to produce detectable LV hypertrophy. TUNEL-positive cardiomyocyte nuclei were increased by approximately eightfold in AAV-control and their number was halved in AAV-VEGF-B, although still higher than normal (Figure 5A and 5B). Consistently, caspase-9 activity was increased and cleaved caspase-3 was clearly detectable only in AAV-control (Figure 5C and 5D).

Oxidative Stress

Total tissue isoprostane content was 37.9±5.4 pg/mg protein in normal LV, increased to 84.0±5.8 pg/mg in AAV-control group ($P<0.05$), but was normalized in paced AAV-VEGF-B (39.3±4.0 pg/mg).

Gene Expression of Murine VEGF-B$_{167}$ and Endogenous VEGF-B$_{167}$, VEGF-A, VEGFR-1, VEGFR-2, and Neuropilin-1

The murine VEGF-B$_{167}$ transgene delivered via AAV was expressed in the injection site and, to a much lesser extent, in the remote site (Online Figure II). However, murine VEGF-B$_{167}$ protein concentration, both in arterial and coronary sinus blood samples, was below the ELISA threshold of detection.

VEGF-A$_{165}$ gene expression was (normalized to Hprt gene expression): 0.87±0.4 in AAV-VEGF-B, 0.63±0.1 in AAV-control ($P<0.05$ versus normal) and 1.05±0.1 in normal, yet VEGF-B$_{\mathbf{167}}$ was not significantly different among groups (data not shown). VEGFR-1 expression was reduced by approximately fourfold and neuropilin-1 by approximately 50% to 30% in both of AAV-control and AAV-VEGF-B compared to normal (Figure 6A). On the other hand, there were no significant differences of VEGFR-2 gene expression among groups.

Activation State of Akt, GSK-3β, and FoxO3a

Protein expression of Akt was not significantly different among groups; however, its phosphorylation was significantly higher in AAV-control compared to normal and even higher in AAV-VEGF-B (Figure 6B). We then examined GSK-3β and FoxO3a, 2 targets of Akt phosphorylation, one cytosolic and the other nuclear, both involved in the control of apoptosis. The levels of protein expression was not significantly different among groups, whereas, inconsistent with Akt hyperactivation, their phosphorylation was significantly reduced in AAV-control compared to normal. In AAV-VEGF-B, however, physiological levels of pospho-GSK-3β were reestablished, whereas phospho-FoxO3a was superphysiological (Figure 6B).

Cultured Cardiac Myocytes

Decreased mitochondrial function in cardiomyocytes is one of the earliest events of Ang II action, which leads to mitochondrial depletion and increased apoptosis. In this regard, we found that Ang II significantly increases apoptosis in cultured cardiac myocytes (Figure 7A), which was consistent with the activation of caspase-9 and -3 (Figure 7B and 7C). Moreover, treatment of cardiac myocytes with Ang II results in significant cellular (Figure 7D) and mitochondrial oxidative stress (Figure 7E through 7G), which are thought to play a role in the induction of apoptotic cell death. Importantly, VEGF-B_{167} effectively protected cardiac myocytes against both Ang II–induced apoptosis (Figure 7A and 7B) and mitochondrial oxidative stress (Figure 7E through 7G). Treatment of cardiac myocytes with Ang II resulted in a loss of red fluorescence of J-aggregates and an increase in green fluorescence of JC-1 monomer (Figure 7H), indicating loss of mitochondrial membrane potential ($\Delta\psi_m$). All of these alterations were attenuated or completely prevented in the presence of VEGF-B_{167}, indicating a preservation of mitochondrial integrity.

Discussion

Our study shows that cardiac delivery of VEGF-B_{167} transgene, obtained by no more than ten direct intramyocardial injections of AAV-9 vectors, delays the progression of pacing-induced dilated cardiomyopathy toward congestive failure. After 4 weeks of tachypacing, hearts transduced with VEGF-B_{167} maintained a LV end-diastolic pressure compatible with physiological pulmonary blood oxygenation, whereas LV wall thickness and global and regional contractile function were either not significantly changed or preserved compared to baseline. On the other hand, VEGF-B_{167} gene transfer did not affect myocardial blood perfusion and oxygen consumption at spontaneous heart rate or during acute pacing stress. Consistently, VEGF-B_{167} transgene did not alter the density of LV microvessels endowed with smooth muscle wall, whereas it prevented the slight capillary rarefaction found in control paced dogs. The low rate of apoptosis and the normalized levels of active capsase-9 and -3 in myocardial tissue suggest antiapoptotic and protrophic actions of VEGF-B_{167}, which likely averted both of cardiomyocyte and capillary endothelial cell loss. Interestingly, the antiapoptotic kinase Akt was more active in the failing heart, as previously found in human and tachypacing-induced heart failure,[33,34] and yet the phosphorylation/inactivation of 2 major targets of this kinase in cytosolic and nuclear compartments, ie, GSK-3β and FoxO3a, known as important proapoptotic mediators,[26–28] was significantly reduced compared to normal hearts. Consistent with its antiapoptotic action, VEGF-B_{167} transduction re-established normal levels of GSK-3β and FoxO3a phosphorylation.

VEGF-B_{167} and Oxidative Stress

The determinants of apoptosis, in the failing heart, are notoriously numerous, and VEGF-B_{167} transgene likely counteracted more than one of them. We focused on oxidative stress, a well recognized cause of myocardial cell damage in various forms of failure,[17,23,24] which is indirectly revealed by fingerprints such as 8-isoprostane and can be triggered by several factors, in particular the locally produced angiotensin II.[30] In paced dogs transduced with VEGF-B_{167}, tissue 8-isoprostane concentration was not significantly different from normal, suggesting a mechanism of protection against oxidative stress. Such mechanism was further tested in cultured cardiomyocytes exposed to angiotensin II: VEGF-B_{167} displayed an action previously unrecognized for this factor, ie, blocked the sequence oxidative stress→mitochondrial damage→apoptosis.[30,31] This adds to cell trophic state enhancement and antiapoptotic effects of VEGF-B_{167} on cultured cardiomyocytes exposed to other insults such as hypoxia/reoxygenation or the genotoxic agent epirubicin, recently shown by us.[9]

Angiogenesis-Unrelated Myocardial Protection

The capability to mitigate the pathogenesis of heart failure without inducing angiogenesis, thus via a direct cytoprotective and protrophic action, has been previously attributed to other families of growth factors, for instance the fibroblast growth factor-5.[35] However, as regards the VEGF family, this is a new paradigm. In fact, the rationale that has thus far driven experimental and clinical protocols with gene delivery of VEGF-A, the best known and most widely used VEGF, in hearts with ischemic[36] and even nonischemic injury,[37] is that the therapeutic outcome of this factor is attributable to neoangiogenesis and consequent perfusion enhancement. However, substantial evidence indicates that the expression of the VEGF receptors VEGFR-1 and -2 is not restricted to endothelial cells, but is present also in other cell types including cardiomyocytes,[9,38] and that their ligand VEGF-A exerts further fundamental functions, beyond proangiogenesis. [1] In a study on VEGF-A_{165} gene transfer to infarcted dog hearts, we observed a functional improvement within 48 hours, a temporal frame not compatible with the formation of new blood vessels and suggestive of a direct protective effect on cardiomyocytes,[38] as proposed also by other authors.[39] More recently, we found that VEGF-B_{167} gene transfer in infarcted rat hearts caused minimal angiogenesis and yet was as much beneficial as VEGF-A.[9] The ensuing question was whether the direct cytoprotective action of a VEGF member, per se, is sufficient to delay the progression of a form of heart failure unrelated to major coronary alterations. The ideal molecular probe to address this question was VEGF-B, a selective ligand of VEGFR-1, not mediating angiogenesis, and therefore devoid of additional, confounding outcomes of new vessel formation in diseased myocardium. Compared to VEGF-A, very little was known about the actions of VEGF-B in response to cell damage until seminal studies published over the past 2 years showed its marked antiapoptotic and cytoprotective effects both in vitro and in vivo.[2,3] These recent findings led us to the hypothesis that cardiac gene transfer of VEGF-B_{167} could ameliorate the evolution of a form of heart failure not caused by tissue loss from ischemic injury. Dilated cardiomyopathy was a well-suited target to test our hypothesis, because, by definition, it is characterized by ventricular chamber dilation in the absence of coronary disease and, independent of its cause that remains in many cases unrecognized, its pathogenesis involves severe cell damage leading to apoptotic death. We used pacing-induced heart failure, a long established model of dilated cardiomyopathy that, although limited as any other model, reproduces many features of the human disease, including cardiomyocyte damage and rate of apoptosis.[17] We now found a further, interesting analogy,[16] ie, decreased gene expression of VEGF-A, but not VEGF-B_{167}, associated with VEGFR-1 and neuopilin-1 downregulation, even in the AAV-VEGF-B group, whereas VEGFR-2 was not significantly altered. This suggests that supplementary, exogenous VEGF-B might have compensated for the reduced availability of its specific receptors VEGFR-1 and neuropilin-1 that, different from VEGFR-2, do not mediate angiogenesis.

Local Versus Global Effects of VEGF-B_{167} Gene Transfer

The method of gene delivery used yielded transduction that was highest in the LV site of injection, and detectable also, albeit much lower, in the remote site. It remains unclear how such nonhomogeneous distribution could affect global LV function, with repercussions on systemic hemodynamics. We could not find measurable levels of mouse VEGF-B_{167} in arterial and coronary sinus blood, ruling out a relevant cell secretion. Nonetheless VEGF-B_{167} gene transfer was sufficient to induce a local increase in the cardiomyocyte cross sectional area, but not as high to determine superphysiological or even untoward structural changes, such as neoangiogenesis and cardiac hypertrophy. Presumably, an excessive VEGF-B_{167} overexpression would have caused marked hypertrophy, as described in transgenic mice.[8] In this regard, it is interesting to note that, in infarcted rabbit and pig hearts, other authors have very recently found therapeutic angiogenesis induced by intracoronary gene delivery of the diffusible isoform VEGF-B_{186} in addition to antiapoptotic effects in cultured cardiomyocytes.[40] Perhaps such difference relative to our results is attributable to the kinetics and dynamics of the diffusible VEGF-B_{186} isoform and/or to the level of its expression and/or to the presence of large areas of ischemia, a condition in which, as proposed by a recent report, this growth factor is critically required for the survival of newly formed vascular cells.[3]

Study Limitations

At least 2 limitations of our study should be pointed out. First, VEGF-B_{167} gene delivery was performed during surgical instrumentation, before and not after starting the pacing protocol, and the study was only in part blinded. However, the present study was not designed as a preclinical trial, as its primary goal was to test VEGF-B_{167}-mediated cardioprotection in a model of progressive cardiac derangement. We needed to minimize confounding variables related to AAV delivery, therefore we chose to use multiple direct intramyocardial injections in well defined points that could be visually identified postmortem in animals that could be operated only once. Nevertheless, no significant differences between groups were noted at baseline, before starting the pacing protocol; furthermore, we recently found VEGF-B_{167} transgene to be effective when administered after and not before inducing myocardial infarction.[9] A second limitation concerns our data on the percent of apoptosis measured by TUNEL-based analysis. Compared to other studies,[14,15,17] it seems overestimated; however, it was not meant to provide an absolute quantification, but rather an index to be interpreted together with other changes such as oxidative stress and caspase activation.

In conclusion, we provide novel evidence that VEGF-B_{167} is a cardiomyocyte protective factor capable of delaying functional derangement in a model of severe cardiomyopathy with high rate of apoptosis, without affecting myocardial blood perfusion and inducing angiogenesis. Besides expanding our knowledge on a relatively undervalued member of the VEGF family, this study has also translational implications, as it suggests a promising new candidate for gene therapy of dilated cardiomyopathy, whose cure, at present, relies on unsatisfactory pharmacological options.

Supplementary Material

Refer to Web version on PubMed Central for supplementary material.

Acknowledgments

Sources of Funding

This study was supported by NIH grants P01-HL-74237 (to F.A.R), P01-HL-43023 (to T.H.H.) and Fondazione CR Trieste (to M.G.). F.A.R. is an Established Investigator of the American Heart Association.

Non-standard Abbreviations and Acronyms

AAV-control	paced dogs transduced with green fluorescent protein
AAV-VEGF-B	paced dogs transduced with VEGF-B_{167}
Ang II	angiotensin II
GFP	green fluorescent protein
GSK	glycogen synthase kinase
LV	left ventricular
MVO_2	myocardial oxygen consumption per minute
VEGF	vascular endothelial growth factor
VEGFR	vascular endothelial growth factor receptor

References

1. Ferrara N, Gerber HP, LeCouter J. The biology of VEGF and its receptors. Nat Med. 2003; 9:669–676. [PubMed: 12778165]
2. Li Y, Zhang F, Nagai N, Tang Z, Zhang S, Scotney P, Lennartsson J, Zhu C, Qu Y, Fang C, Hua J, Matsuo O, Fong GH, Ding H, Cao Y, Becker KG, Nash A, Heldin CH, Li X. VEGF-B inhibits apoptosis via VEGFR-1-mediated suppression of the expression of BH3-only protein genes in mice and rats. J Clin Invest. 2008; 118:913–923. [PubMed: 18259607]
3. Zhang F, Tang Z, Hou X, Lennartsson J, Li Y, Koch AW, Scotney P, Lee C, Arjunan P, Dong L, Kumar A, Rissanen TT, Wang B, Nagai N, Fons P, Fariss R, Zhang Y, Wawrousek E, Tansey G, Raber J, Fong GH, Ding H, Greenberg DA, Becker KG, Herbert JM, Nash A, Yla-Herttuala S, Cao Y, Watts RJ, Li X. VEGF-B is dispensable for blood vessel growth but critical for their survival, and VEGF-B targeting inhibits pathological angiogenesis. Proc Natl Acad Sci U S A. 2009; 106:6152–6157. [PubMed: 19369214]
4. Olofsson B, Pajusola K, Kaipainen A, von Euler G, Joukov V, Saksela O, Orpana A, Pettersson RF, Alitalo K, Eriksson U. Vascular endothelial growth factor B, a novel growth factor for endothelial cells. Proc Natl Acad Sci U S A. 1996; 93:2576–2581. [PubMed: 8637916]
5. Li X, Aase K, Li H, von Euler G, Eriksson U. Isoform-specific expression of VEGF-B in normal tissues and tumors. Growth Factors. 2001; 19:49–59. [PubMed: 11678209]
6. Bellomo D, Headrick JP, Silins GU, Paterson CA, Thomas PS, Gartside M, Mould A, Cahill MM, Tonks ID, Grimmond SM, Townson S, Wells C, Little M, Cummings MC, Hayward NK, Kay GF. Mice lacking the vascular endothelial growth factor-B gene (Vegfb) have smaller hearts, dysfunctional coronary vasculature, and impaired recovery from cardiac ischemia. Circ Res. 2000; 86:e29–e35. [PubMed: 10666423]

7. Aase K, von Euler G, Li X, Ponten A, Thoren P, Cao R, Cao Y, Olofsson B, Gebre-Medhin S, Pekny M, Alitalo K, Betsholtz C, Eriksson U. Vascular endothelial growth factor-B-deficient mice display an atrial conduction defect. Circulation. 2001; 104:358–364. [PubMed: 11457758]
8. Karpanen T, Bry M, Ollila HM, Seppanen-Laakso T, Liimatta E, Leskinen H, Kivela R, Helkamaa T, Merentie M, Jeltsch M, Paavonen K, Andersson LC, Mervaala E, Hassinen IE, Yla-Herttuala S, Oresic M, Alitalo K. Overexpression of vascular endothelial growth factor-B in mouse heart alters cardiac lipid metabolism and induces myocardial hypertrophy. Circ Res. 2008; 103:1018–1026. [PubMed: 18757827]
9. Zentilin L, Puligadda U, Lionetti V, Zacchigna S, Collesi C, Pattarini L, Ruozi G, Camporesi S, Sinagra G, Pepe M, Recchia FA, Giacca M. Cardiomyocyte VEGFR-1 activation by VEGF-B induces compensatory hypertrophy and preserves cardiac function after myocardial infarction. FASEB J. In press.
10. Everly MJ. Cardiac transplantation in the United States: an analysis of the UNOS registry. Clin Transpl. 2008:35–43. [PubMed: 19708444]
11. Narula J, Haider N, Virmani R, DiSalvo TG, Kolodgie FD, Hajjar RJ, Schmidt U, Semigran MJ, Dec GW, Khaw BA. Apoptosis in myocytes in end-stage heart failure. N Engl J Med. 1996; 335:1182–1189. [PubMed: 8815940]
12. Olivetti G, Abbi R, Quaini F, Kajstura J, Cheng W, Nitahara JA, Quaini E, Di Loreto C, Beltrami CA, Krajewski S, Reed JC, Anversa P. Apoptosis in the failing human heart. N Engl J Med. 1997; 336:1131–1141. [PubMed: 9099657]
13. Saraste A, Pulkki K, Kallajoki M, Heikkilä P, Laine P, Mattila S, Nieminen MS, Parvinen M, Voipio-Pulkki LM. Cardiomyocyte apoptosis and progression of heart failure to transplantation. Eur J Clin Invest. 1999; 29:380–386. [PubMed: 10354194]
14. Wencker D, Chandra M, Nguyen K, Miao W, Garantziotis S, Factor SM, Shirani J, Armstrong RC, Kitsis RN. A mechanistic role for cardiac myocyte apoptosis in heart failure. J Clin Invest. 2003; 111:1497–1504. [PubMed: 12750399]
15. Yamamoto S, Yang G, Zablocki D, Liu J, Hong C, Kim SJ, Soler S, Odashima M, Thaisz J, Yehia G, Molina CA, Yatani A, Vatner DE, Vatner SF, Sadoshima J. Activation of Mst1 causes dilated cardiomyopathy by stimulating apoptosis without compensatory ventricular myocyte hypertrophy. J Clin Invest. 2003; 111:1463–1474. [PubMed: 12750396]
16. Abraham D, Hofbauer R, Schäfer R, Blumer R, Paulus P, Miksovsky A, Traxler H, Kocher A, Aharinejad S. Selective downregulation of VEGF-A(165), VEGF-R(1), and decreased capillary density in patients with dilative but not ischemic cardiomyopathy. Circ Res. 2000; 87:644–647. [PubMed: 11029398]
17. Cesselli D, Jakoniuk I, Barlucchi L, Beltrami AP, Hintze TH, Nadal-Ginard B, Kajstura J, Leri A, Anversa P. Oxidative stress-mediated cardiac cell death is a major determinant of ventricular dysfunction and failure in dog dilated cardiomyopathy. Circ Res. 2001; 89:279–286. [PubMed: 11485979]
18. Pacak CA, Mah CS, Thattaliyath BD, Conlon TJ, Lewis MA, Cloutier DE, Zolotukhin I, Tarantal AF, Byrne BJ. Recombinant adeno-associated virus serotype 9 leads to preferential cardiac transduction in vivo. Circ Res. 2006; 99:e3–e9. [PubMed: 16873720]
19. Recchia FA, McConnell PI, Bernstein RD, Vogel TR, Xu X, Hintze TH. Reduced nitric oxide production and altered myocardial metabolism during the decompensation of pacing-induced heart failure in the conscious dog. Circ Res. 1998; 83:969–979. [PubMed: 9815144]
20. Qanud K, Mamdani M, Pepe M, Khairallah RJ, Gravel J, Lei B, Gupte SA, Sharov VG, Sabbah HN, Stanley WC, Recchia FA. Reverse changes in cardiac substrate oxidation in dogs recovering from heart failure. Am J Physiol. 2008; 295:H2098–H2105.
21. Lei B, Matsuo K, Labinskyy V, Sharma N, Chandler MP, Ahn A, Hintze TH, Stanley WC, Recchia FA. Exogenous nitric oxide reduces glucose transporters translocation and lactate production in ischemic myocardium in vivo. Proc Natl Acad Sci U S A. 2005; 102:6966–6971. [PubMed: 15870202]
22. Zacchigna S, Pattarini L, Zentilin L, Moimas S, Carrer A, Sinigaglia M, Arsic N, Tafuro S, Sinagra G, Giacca. Bone marrow cells recruited through the Neuropilin-1 receptor promote arterial formation at the sites of adult neoangiogenesis. J Clin Invest. 2008; 118:2062–2075. [PubMed: 18483621]

23. Heymes C, Bendall JK, Ratajczak P, Cave AC, Samuel JL, Hasenfuss G, Shah AM. Increased myocardial NADPH oxidase activity in human heart failure. J Am Coll Cardiol. 2003; 41:2164–2171. [PubMed: 12821241]

24. Gupte RS, Vijay V, Marks B, Levine RJ, Sabbah HN, Wolin MS, Recchia FA, Gupte SA. Upregulation of glucose-6-phosphate dehydrogenase and NAD(P)H oxidase activity increases oxidative stress in failing human heart. J Card Fail. 2007; 13:497–506. [PubMed: 17675065]

25. Matsui T, Li L, del Monte F, Fukui Y, Franke TF, Hajjar RJ, Rosenzweig A. Adenoviral gene transfer of activated phosphatidylinositol 3′-kinase and Akt inhibits apoptosis of hypoxic cardiomyocytes in vitro. Circulation. 1999; 100:2373–2379. [PubMed: 10587343]

26. Pap M, Cooper G. Role of glycogen synthase kinase-3 in the phosphatidylinositol 3-kinase/Akt cell survival pathway. J Biol Chem. 1998; 273:19929–19932. [PubMed: 9685326]

27. Shiraishi I, Melendez J, Ahn Y, Skavdahl M, Murphy E, Welch S, Schaefer E, Walsh K, Rosenzweig A, Torella D, Nurzynska D, Kajstura J, Leri A, Anversa P, Sussman MA. Nuclear targeting of Akt enhances kinase activity and survival of cardiomyocytes. Circ Res. 2004; 94:884–891. [PubMed: 14988230]

28. Webster KA. Aktion in the nucleus. Circ Res. 2004; 94:856–859. [PubMed: 15087424]

29. Serneri GG, Boddi M, Cecioni I, Vanni S, Coppo M, Papa ML, Bandinelli B, Bertolozzi I, Polidori G, Toscano T, Maccherini M, Modesti PA. Cardiac angiotensin II formation in the clinical course of heart failure and its relationship with left ventricular function. Circ Res. 2001; 88:961–968. [PubMed: 11349007]

30. Kajstura J, Bolli R, Sonnenblick EH, Anversa P, Leri A. Cause of death: suicide. J Mol Cell Cardiol. 2006; 40:425–437. [PubMed: 16513132]

31. Doughan AK, Harrison DG, Dikalov SI. Molecular mechanisms of angiotensin II-mediated mitochondrial dysfunction: linking mitochondrial oxidative damage and vascular endothelial dysfunction. Circ Res. 2008; 102:488–496. [PubMed: 18096818]

32. Csiszar A, Labinskyy N, Perez V, Recchia FA, Podlutsky A, Mukhopadhyay P, Losonczy G, Pacher P, Austad SN, Bartke A, Ungvari Z. Endothelial function and vascular oxidative stress in long-lived GH/IGF-deficient Ames dwarf mice. Am J Physiol. 2008; 295:H1882–H1894.

33. Haq S, Choukroun G, Lim H, Tymitz KM, del Monte F, Gwathmey J, Grazette L, Michael A, Hajjar R, Force T, Molkentin JD. Differential activation of signal transduction pathways in human hearts with hypertrophy versus advanced heart failure. Circulation. 2001; 103:670–677. [PubMed: 11156878]

34. Sasaki H, Asanuma H, Fujita M, Takahama H, Wakeno M, Ito S, Ogai A, Asakura M, Kim J, Minamino T, Takashima S, Sanada S, Sugimachi M, Komamura K, Mochizuki N, Kitakaze M. Metformin prevents progression of heart failure in dogs: role of AMP-activated protein kinase. Circulation. 2009; 119:2568–2577. [PubMed: 19414638]

35. Suzuki G, Lee TC, Fallavollita JA, Canty JM Jr. Adenoviral gene transfer of FGF-5 to hibernating myocardium improves function and stimulates myocytes to hypertrophy and reenter the cell cycle. Circ Res. 2005; 96:767–775. [PubMed: 15761196]

36. Losordo DW, Vale PR, Hendel RC, Milliken CE, Fortuin FD, Cummings N, Schatz RA, Asahara T, Isner JM, Kuntz RE. Phase 1/2 placebocontrolled, double-blind, dose-escalating trial of myocardial vascular endothelial growth factor 2 gene transfer by catheter delivery in patients with chronic myocardial ischemia. Circulation. 2002; 105:2012–2018. [PubMed: 11980678]

37. Leotta E, Patejunas G, Murphy G, Szokol J, McGregor L, Carbray J, Hamawy A, Winchester D, Hackett N, Crystal R, Rosengart T. Gene therapy with adenovirus-mediated myocardial transfer of vascular endothelial growth factor 121 improves cardiac performance in a pacing model of congestive heart failure. J Thorac Cardiovasc Surg. 2002; 123:1101–1113. [PubMed: 12063456]

38. Ferrarini M, Arsic N, Recchia FA, Zentilin L, Zacchigna S, Xu X, Linke A, Giacca M, Hintze TH. 1. Adeno-associated virus-mediated transduction of VEGF165 improves cardiac tissue viability and functional recovery after permanent coronary occlusion in conscious dogs. Circ Res. 2006; 98:954–961. [PubMed: 16543500]

39. Laguens R, Cabeza Meckert P, Vera Janavel G, Del Valle H, Lascano E, Negroni J, Werba P, Cuniberti L, Martinez V, Melo C, Papouchado M, Ojeda R, Criscuolo M, Crottogini A. Entrance in

mitosis of adult cardiomyocytes in ischemic pig hearts after plasmid-mediated rhVEGF165 gene transfer. Gene Ther. 2002; 9:1676–1681. [PubMed: 12457281]

40. Lähteenvuo JE, Lähteenvuo MT, Kivelä A, Rosenlew C, Falkevall A, Klar J, Heikura T, Rissanen TT, Vähäkangas E, Korpisalo P, Enholm B, Carmeliet P, Alitalo K, Eriksson U, Ylä-Herttuala S. Vascular endothelial growth factor-B induces myocardium-specific angiogenesis and arteriogenesis via vascular endothelial growth factor receptor-1- and neuropilin receptor-1-dependent mechanisms. Circulation. 2009; 119:845–856. [PubMed: 19188502]

Author Manuscript
Author Manuscript
Author Manuscript

Author Manuscript

Author Manuscript

Author Manuscript

Novelty and Significance

What Is Known?

- Vascular endothelial growth factor (VEGF)-B, a selective ligand of the receptor VEGFR-1, is a minimally angiogenic growth factor that plays an important role in heart development and, when overexpressed, induces cardiomyocyte hypertrophy.
- The isoforms VEGF-B_{167} and VEGF-B_{186} can activate potent cytoprotective mechanisms in cells exposed to a variety of harmful conditions.
- VEGF-B exerts a marked cardioprotective effect in ischemic/infarcted hearts by binding VEGFR-1 expressed by cardiomyocytes.

What New Information Does This Article Contribute?

- VEGF-B_{167} gene delivery to the heart delays ventricular pump failure in a dog model of nonischemic dilated cardiomyopathy, while not inducing significant neoangiogenesis.
- VEGF-B_{167} attenuates oxidative stress and apoptosis, 2 interrelated, major determinants of progressive tissue loss in nonischemic dilated cardiomyopathy.
- Consistent with its cytoprotective effects in failing hearts, VEGF-B_{167} prevents oxidative stress and mitochondrial damage caused by angiotensin II in cultured cardiomyocyte.

VEGF-B is emerging as a major cytoprotective factor; however, no previous studies had tested its beneficial effects in nonischemic cardiac diseases. VEGF-B_{167} cDNA carried by adeno-associated viral vectors was delivered to the myocardium of dogs developing tachypacing-induced dilated cardiomyopathy. After 4 weeks of pacing, these dogs were still in a well-compensated state compared to control dogs. Consistently, hemodynamic and cardiac functional and morphological parameters were better preserved. Histological and molecular analysis indicated that VEGF-B_{167} markedly attenuated oxidative stress and cell apoptosis without inducing detectable neoangiogenesis. The cytoprotective effects of VEGF-B_{167} were further elucidated in cultured rat neonatal cardiomyocytes exposed to high concentrations of angiotensin II to mimic a recognized cause of oxidative stress and cell damage occurring in failing hearts. VEGF-B_{167} prevented oxidative stress, loss of mitochondrial membrane potential, and, consequently, apoptosis. We provide novel evidence that VEGF-B_{167} is a cardiomyocyte protective factor capable of delaying the onset of decompensated failure in a model of severe nonischemic cardiomyopathy, without altering myocardial vascularization. Besides expanding our knowledge of a less known member of the VEGF family, this study has also translational implications, because it suggests a promising new candidate for gene therapy of dilated cardiomyopathy, whose cure, at present, relies on unsatisfactory pharmacological options.

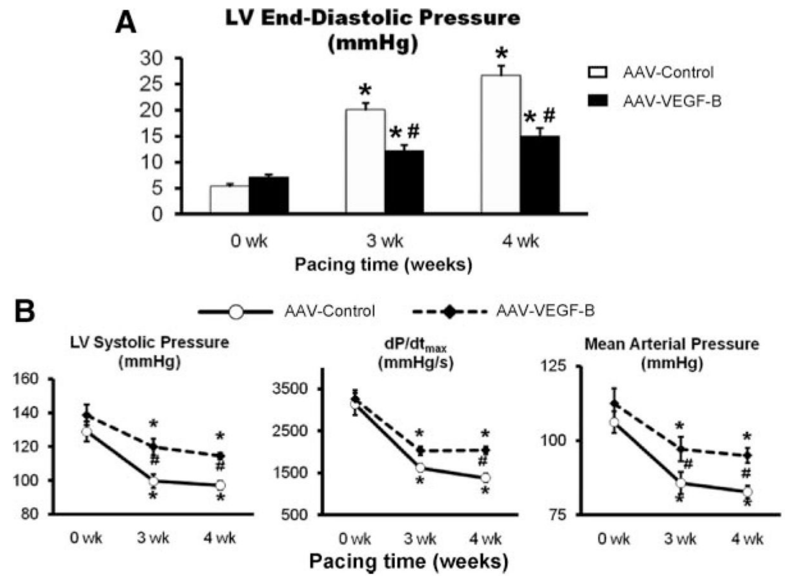

Figure 1. Changes in major hemodynamic parameters over the 4 weeks of chronic pacing

A, Changes in LV end-diastolic pressure. **B,** Changes in LV systolic pressure, dP/dtmax and mean arterial pressure. n=8 per group. Measurements were taken with the pacemaker off. ***** *P*<0.05 vs 0 weeks (baseline) within the group; #*P*<0.05 between groups at same time point.

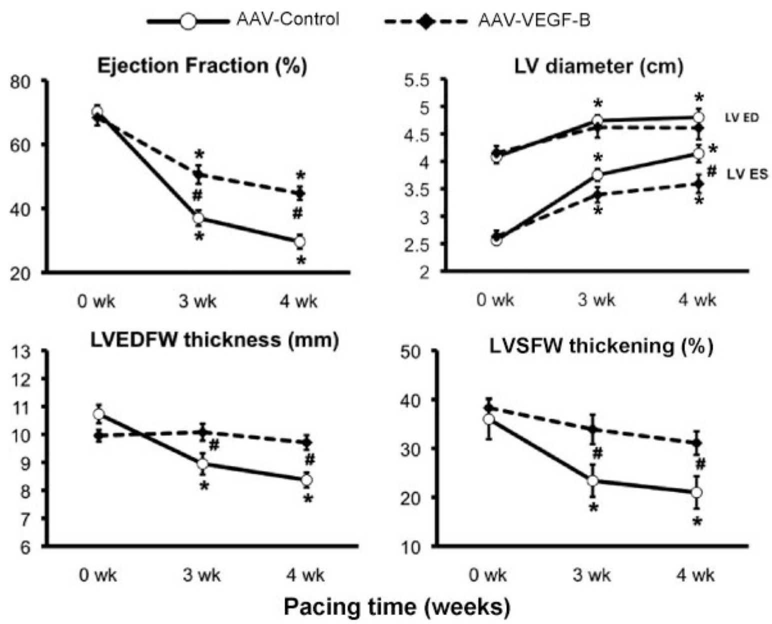

Figure 2. Changes in echocardiographic parameters over the 4 weeks of chronic pacing

LVED indicates LV end-diastolic; ED, end-diastolic; ES, end-systolic; LVEDFW, end-diastolic thickness of the LV free wall; LVSFW, LV systolic free wall. Measurements were taken with the pacemaker off. ***P<0.05 vs 0 weeks (baseline) within the group; #P<0.05 between groups at same time point; n=8 per group.

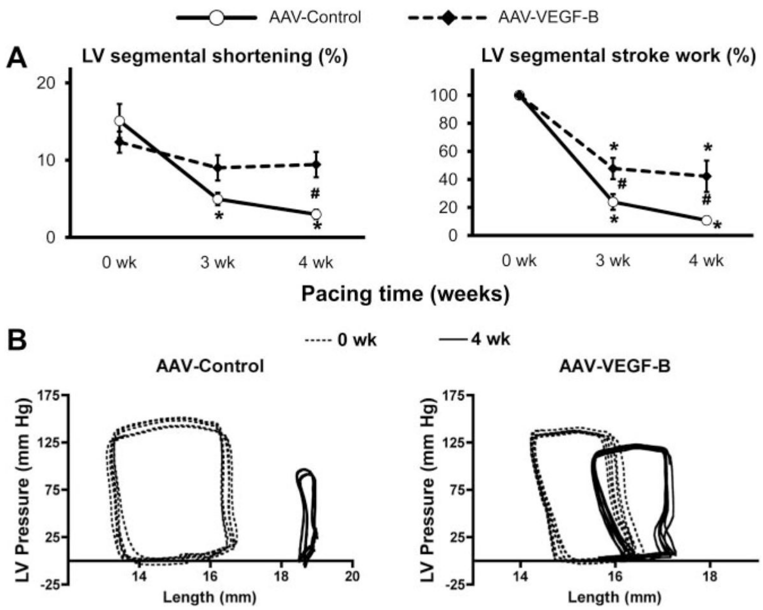

Figure 3. Regional contractile function

A, Changes in 2 indexes of regional contractile function calculated from cyclic variations of the LV distance (segmental length) between piezoelectric crystals implanted in the LV free wall. The surrogate of the regional stroke work was obtained as the area of the LV pressure–segmental length loop and normalized to baseline (n=8 per group). Measurements were taken with the pacemaker off. ***P<0.05 vs 0 weeks (baseline) within the group and #P<0.05 between groups at same time point. **B,** Representative pressure-length loops at 0 and 4 weeks pacing.

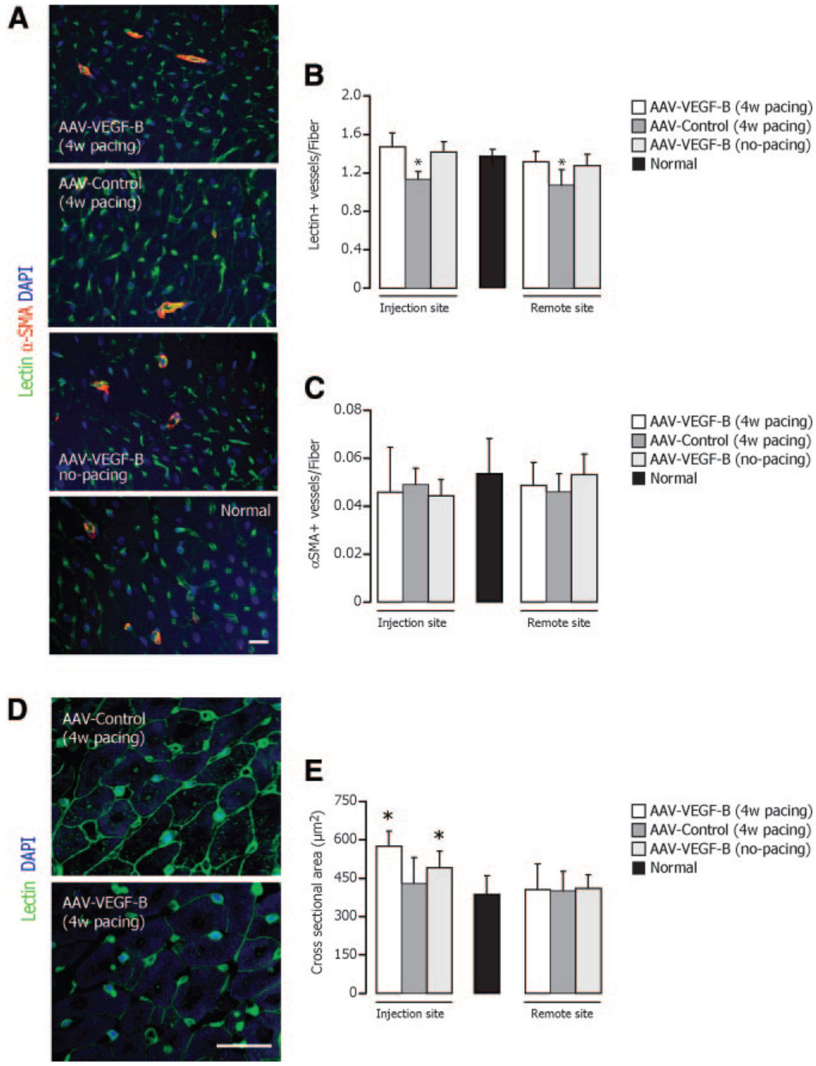

Figure 4. Microscopic analysis of angiogenesis and cardiomyocyte hypertrophy

A, Representative photomicrographs of myocardial tissue showing double immunofluorescence staining for endothelial cells (lectin$^+$, green), vascular smooth muscle cells (α-SMA$^+$) **(red)**, whereas nuclei were stained with DAPI **(blue). B and C,** Microvessel density was normalized by the number of cardiomyocyte fibers. **D and E,** FITC-conjugated lectin **(green)** was used to stain myocardium and quantify cardiomyocyte cross-sectional area. *P<0.05 vs normal; n=6 per group.

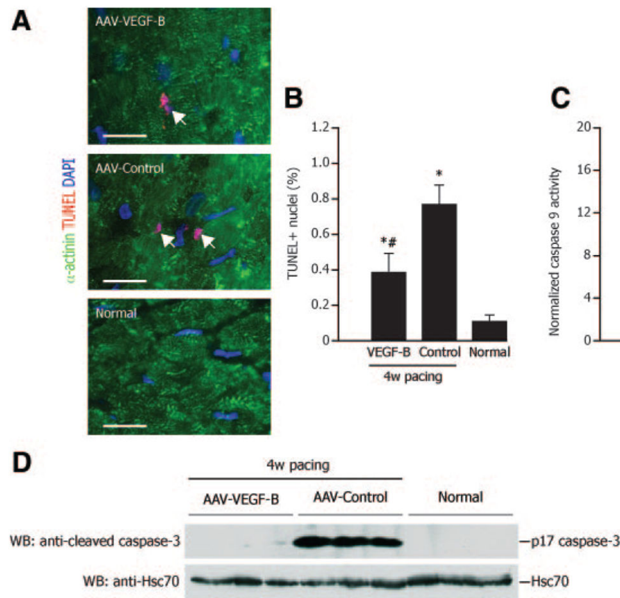

Figure 5. VEGF-B$_{167}$ protects myocardium from apoptosis

A and B, Cardiomyocyte apoptotic nuclei **(white arrows)** by TUNEL **(red)** analysis. Cardiomyocytes are stained with *α*-actinin **(green). Bars:** #*P*<0.05 vs AAV-control; n=4 per group. **D,** Representative Western blotting analysis of activated/cleaved caspase-3 (17 kDa). The bands were not detectable in normal and AAV-VEGF-B, indicating virtually no cleavage.

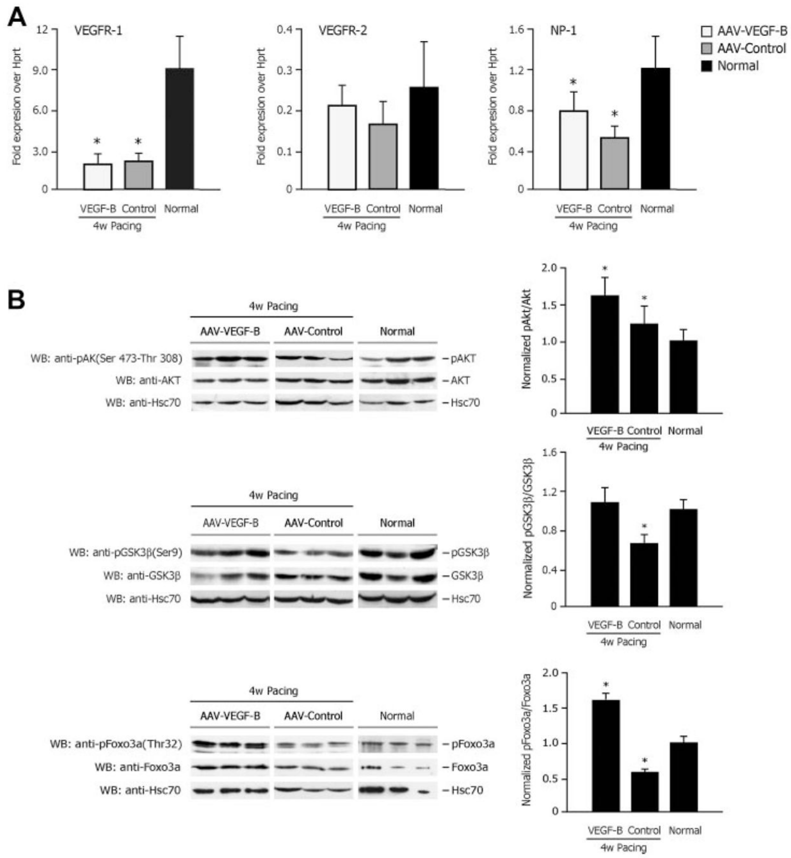

Figure 6. VEGF receptor expression and activation of Akt, GSK-3*β*, and FoxO3a

A, Real-time PCR quantification of VEGFR-1, VEGFR-2, and neuropilin-1 (NP-1) gene expression. **B,** Western blotting analysis of activating phosphorylation of Akt and inactivating phosphorylation of its down-stream targets GSK-3*β* and FoxO3a. **P*<0.05 vs normal; n=6 per group.

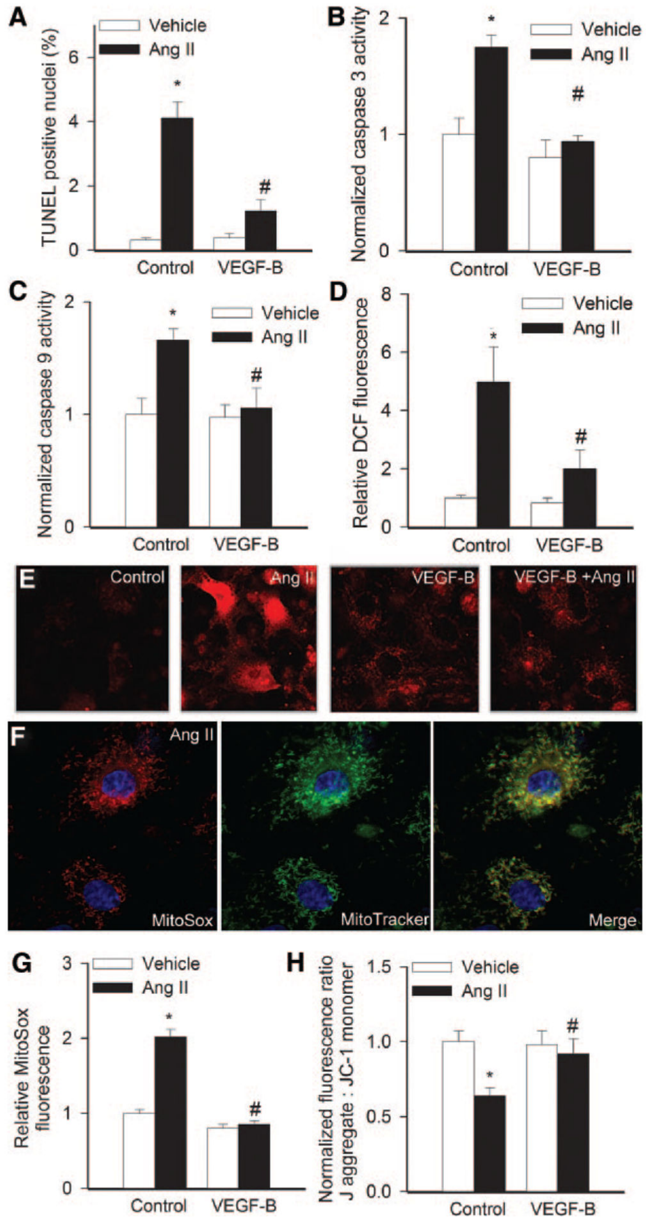

Figure 7. VEGF-B$_{167}$ protects cardiomyocytes from Ang II-induced apoptosis

Percentage of TUNEL-positive nuclei **(A)**, caspase-3 and -9 activity normalized by protein concentration **(B and C)** and cellular peroxide levels **(D)** in rat neonatal cardiac myocytes treated with Ang II (10^{-8} mol/L) with or without VEGF-B$_{167}$. **E,** Representative fluorescent images showing stronger MitoSox staining **(red fluorescence)** in Ang II–treated cardiac myocytes than in untreated controls (note also the increased number of early apoptotic cells exhibiting nuclear accumulation of MitoSox). VEGF-B$_{167}$ substantially attenuated MitoSox fluorescence in Ang II–treated cells (original magnification, ×40). **F,** Increased MitoSox staining localizes to the perinuclear mitochondria (counterstained with Mito- Tracker green) of nonapoptotic Ang II–treated cardiac myocytes (**blue fluorescence**: nuclear counterstaining). **G and H,** Summary of flow cytometric data showing relative MitoSox fluorescence **(E)** and J-aggregate: JC-1 monomer fluorescence ratios in rat neonatal cardiac myocytes treated with Ang II (10^{-8} mol/L) with or without pretreatment with VEGF-B. Data are means±SEM (n=6). *P<0.05 vs no Ang II; #P<0.05 vs no VEGF-B_{167}.

Table

Blood Flow in the Left Circumflex Coronary Artery in Myocardial Perfusion and in Cardiac Oxygen Consumption

	0 Weeks (Pacing Off)		0 Weeks (Acute Pacing)		4 Weeks (Pacing Off)		4 Weeks (Acute Pacing)	
	AAV-Control	AAV-VEGF-B	AAV-Control	AAV-VEGF-B	AAV-Control	AAV-VEGF-B	AAV-Control	AAV-VEGF-B
LCx CBF (mL/min)	33.14±4.03	35.63±2.91	43.64±6.37*	44.62±2.87*	34.12±4.12	31.50±2.25	41.34±5.45*	38.99±3.77*
Myocardial perfusion (mL/min/g)	1.03±0.08	1.10±0.15	1.88±0.28*	1.75±0.16*	1.23±0.06	1.15±0.20	1.76±0.20*	1.73±0.17*
MVO_2 (mL/min)	6.72±0.68	8.18±0.40	8.62±0.64*	12.06±1.24*	6.9±0.34	7.9±0.56	8.96±0.62*	9.52±1.68*

Blood flow in the left circumflex coronary artery (Lcx CBF), myocardial perfusion assessed by microsphere infusion, and cardiac oxygen consumption measured at 0 weeks and at 4 weeks pacing, both at spontaneous heart rate (pacing off) and during acute (10 minutes) pacing stress (n=6–8 per group).

* $P<0.05$ of acute pacing vs pacing off.